



1 **Searching for an optimized single-objective function**
2 **matching multiple objectives with automatic calibration of**
3 **hydrological models**

4 Fuqiang Tian^{1*}, Yu Sun¹, Hongchang Hu¹, Hongyi Li²

5

6 1 Department of Hydraulic Engineering, State Key Laboratory of Hydrosience and
7 Engineering, Tsinghua University, Beijing 100084, China

8 2 Pacific Northwest National Laboratory, P.O. Box 999, Richland, WA 99352, USA

9

10 *Corresponding author information:

11 Email: tianfq@tsinghua.edu.cn

12 Telephone: +86 010 6277 3396

13 Fax: +86 010 6279 6971

14

15

16

17

18 Submitted to Hydrology and Earth System Sciences

19 February 22, 2016

20



21 **Abstract:**

22 In the calibration of hydrological models, evaluation criteria are explicitly and quantitatively
23 defined as single- or multi-objective functions when utilizing automatic calibration approaches. In
24 most previous studies, there is a general opinion that no single-objective function can represent all
25 of the important characteristics of even one specific kind of hydrological variable (e.g.,
26 streamflow). Thus hydrologists must turn to multi-objective calibration. In this study, we
27 demonstrated that an optimized single-objective function can compromise multi-response modes
28 (i.e., multi-objective functions) of the hydrograph, which is defined as summation of a power
29 function of the absolute error between observed and simulated streamflow with the exponent of
30 power function optimized for specific watersheds. The new objective function was applied to 196
31 model parameter estimation experiment (MOPEX) watersheds across the eastern United States
32 using the semi-distributed Xinanjiang hydrological model. The optimized exponent value for each
33 watershed was obtained by targeting four popular objective functions focusing on peak flows, low
34 flows, water balance, and flashiness, respectively. The results showed that the optimized
35 single-objective function can achieve a better hydrograph simulation compared to the traditional
36 single-objective function Nash-Sutcliffe efficiency coefficient for most watersheds, and balance
37 high flow part and low flow part of the hydrograph without substantial differences compared to
38 multi-objective calibration. The proposed optimal single-objective function can be practically
39 adopted in the hydrological modeling if the optimal exponent value could be determined *a priori*
40 according to hydrological/climatic/landscape characteristics in a specific watershed. This is,
41 however, left for future study.



42 **Keywords:** automatic calibration, single-objective function, multi-objective functions,
43 hydrological model

44 **1. Introduction**

45 Hydrological models are often used to simulate the past and to predict the future hydrological
46 behaviors of catchment. All kinds of models, lumped conceptual models or distributed physically
47 based models, are simplifications of reality. Their parameters usually cannot be directly observed
48 or easily derived from measurable catchment characteristics, but have to be indirectly estimated by
49 some kind of calibration methods (Booij and Krol, 2010; Madsen, 2000; Pokhrel and Gupta, 2010;
50 Vrugt et al., 2002). Calibration means that parameters are adjusted to match model simulation with
51 historically observed data as closely as possible. Generally, it is translated into an optimization
52 problem from the perspective of mathematics, and performed automatically using optimization
53 algorithms (Guinot et al., 2011; Muleta, 2012). In this approach, objective functions are necessary
54 to evaluate the closeness between the simulated and observed variable.

55 There are ample literatures on model performance evaluation, because it is important not only
56 for calibration but also for model development and intercomparison (Krause et al., 2005; Muleta,
57 2012; Wagener, 2003). The traditional approach is using a single-objective function. However,
58 many researchers share the concerns about single-objective functions such as the most widely
59 used Nash-Sutcliffe efficiency (NSE) (Jain and Sudheer, 2008; McCuen et al., 2006; Schaeffli and
60 Gupta, 2007). The opinion that a single-objective function cannot capture all of the important
61 characteristics of the observed data has been gradually accepted (Vrugt et al., 2003; Wagener,
62 2003). More and more hydrologists seek to improve the calibration methods to capture various
63 aspects of hydrologic responses simultaneously (Fenicia et al., 2007; Madsen et al., 2002).



64 Inspired by the excellent studies by Gupta et al. (1998) and Yapo et al. (1998), multi-objective
65 calibration has been considered to be able to extract more information from historical data hence
66 widely used to identify non-dominated or Pareto optimal parameter sets (Gupta et al., 2009; Hall
67 et al., 2005; Matott et al., 2009; van Werkhoven et al., 2009). The progress in multi-objective
68 calibration in recent years was well summarized in a comprehensive review paper by Efstratiadis
69 and Koutsoyiannis (2010).

70 In general, multi-objective calibration can be categorized into three types, i.e., multiple
71 objectives based on multi-variable measurements, multi-site measurements, and multi-response
72 modes (Madsen, 2003). In this study, multi-objective calibration referred to the third type that
73 measures various responses of the hydrological processes, especially the streamflow hydrograph.
74 High flows and low flows are two important characteristics of the hydrograph and the trade-offs
75 between them have been considerably discussed (Bekele and Nicklow, 2007; Boyle et al., 2000;
76 Gill et al., 2006; Khu et al., 2008; Tang et al., 2007; van Griensven and Bauwens, 2003). In
77 addition, water balance and flow variability are of great importance as well (Kollat et al., 2012;
78 Price et al., 2012; van Werkhoven et al., 2009).

79 The multi-objective calibration produces a series of parameter sets located on the Pareto front,
80 which provides new perspectives for parameter estimation. However, single-objective calibration
81 has still been widely used, because a unique parameter set is often preferred by decision makers
82 for daily water resources management practices. It is useful to identify a good compromise against
83 the conflicting objectives. For this purpose, in this study we proposed a new methodology to
84 obtain an optimized single-objective function (OSOF) which can simultaneously address
85 multi-response modes for automatic calibration of hydrological models.



86 This paper was organized as follows. After this brief introduction, in Section 2, we
87 introduced the definition of new single-objective function. Case study areas and data, the applied
88 methods including the hydrological model, the optimization algorithm, the evaluation framework,
89 and the procedure of numerical experiments were presented in Section 3. Then in Section 4, we
90 showed the optimized single-objective function for the study areas, compared with traditional
91 single-objective function NSE and multi-objective calibration. Finally, conclusions were drawn in
92 Section 5.

93 **2. Definition of objective function**

94 Most objective functions used for calibration of hydrological models contain a summation of the
95 error term, i.e. the difference between the simulated and observed variable (Krause et al., 2005). In
96 addition, absolute or square function is introduced to avoid the offset between errors with opposite
97 signs. In order to normalize the objective function, a baseline or benchmark, such as average of
98 observed variables, is often used in many objective functions. As the average of observed
99 variables is a constant value, such linear normalization has no impact on the calibration results.
100 Therefore, only the power function of absolute errors is of major importance for model calibration.

101 Different exponent value of the objective function leads to emphasizing different
102 hydrological response mode in the calibration. For example, the exponent value of NSE function
103 is 2 (see Eq. (2) below). When we try to maximize NSE to find the best parameter set of a
104 hydrological model, it leads to matching high flow parts of the hydrograph at the expense of low
105 flow parts, because errors related to high flows are amplified and tend to be larger than those
106 related to low flows. Conversely, if the exponent is smaller, errors related to low flows tend to be



107 relatively emphasized and low flows can thus be better replicated.

108 Based on the above analysis, we proposed a hypothesis that appropriate (optimal) exponent
109 value can balance multi-response modes of the hydrograph. To explore the optimal exponent value
110 (OEV), a general form of the new single-objective function is defined as,

$$111 \quad C = \sum_{t=1}^n |Q_{s,t} - Q_{o,t}|^b \quad (1)$$

112 where, C is the newly proposed single-objective evaluation criterion, $Q_{s,t}$ is the simulated
113 streamflow at time t , $Q_{o,t}$ is the observed streamflow at time t , n is the length of entire
114 simulation period. Given a specific watershed and a proper hydrological model, there is an optimal
115 exponent b with which the proposed objective function can simultaneously address multi-response
116 modes of the hydrograph. We call the objective function with the exponent value of OEV the
117 optimal single-objective function (OSOF). Practical hydrological modeling experience suggests
118 that NSE is an appropriate objective function for replicating high flows, thus the exponent b was
119 assumed less than or equal to 2 in this study. Here we take streamflow as a demonstrating
120 hydrological variable, but one can easily extend to other variables in the future study.

121 3. Materials and Methods

122 3.1 Hydrological model

123 In this study, the Xinanjiang model (Zhao, 1992) was used as a runoff generation module, the
124 Model for Scale Adaptive River Transport (MOSART) (Li et al., 2013) was used as a routing
125 module. The Xinanjiang model was proposed in 1973 and is based on the concept of runoff
126 formation on repletion of storage. The runoff generation is composed of three components: surface,
127 subsurface, and groundwater, which are calculated based on tension water capacity and free water



128 capacity. Based on soil moisture and potential evapotranspiration, the evapotranspiration is
 129 calculated from three vertical layers. This model has been widely used in humid and semi-humid
 130 watersheds (Bao et al., 2011; Cheng et al., 2006; Gan et al., 1997; Ju et al., 2009; Li et al., 2009;
 131 Zhao, 1992), and cannot be used in watersheds where snow processes is of importance because it
 132 has no snow module. Two criteria, therefore, need to be satisfied for the watersheds used in this
 133 study: the climate is humid or semi-humid, and snow processes can be ignored.

134 A runoff routing model, called MOSART, was developed by Li et al. (2013) and has been
 135 applied at different spatial resolutions. In this model, surface runoff was assumed to be first routed
 136 across hillslopes and then discharged along with subsurface runoff into a sub-network channel
 137 before entering the main channel. The sub-network channel is a hypothetical equivalent to all
 138 tributaries combined, i.e., with equivalent transport capacity. For the hillslope and sub-network
 139 channel routing, the kinematic wave routing method is used. For the main channel routing, both
 140 kinematic and diffusion wave routing methods are available, but the former was used in this study.

141 In summary, the hydrological model has 14 calibrated parameters: 5 parameters related to
 142 evaporation, i.e., K, C, WUM, WLM, WDM; 2 parameters related to runoff generation, i.e., B,
 143 IMP; 4 parameters related to runoff partition, i.e., SM, EX, KG, KSS; and 3 parameters related to
 144 runoff routing, i.e., C_nh, C_nr, C_twidth. The physical meaning of the model parameters and the
 145 range of parameter values were given in Table 1.

146 Table 1. Parameters of the hydrological model

Parameter	Physical meaning	Unit	Range
K	Evaporation pan coefficient	-	0.70-0.99
C	Coefficient of the deep layer, that depends on the proportion of the basin area covered by vegetation with deep roots	-	0.1-0.4
WUM	Averaged soil moisture capacity of the upper layer	mm	5-120



WLM	Averaged soil moisture capacity of the lower layer	mm	5-120
WDM	Averaged soil moisture capacity of the deep layer	mm	5-120
B	Representation of the non-uniformity of the spatial distribution of soil moisture storage capacity over the watershed	-	0.1-0.7
IMP	Percentage of impervious and saturated areas in the watershed	-	0-0.05
SM	Areal mean free water capacity of the surface soil layer, which represents the maximum possible deficit of free water storage	mm	1-30
EX	Exponent of the free water capacity curve influencing the development of the saturated area	-	0-2
KG	Outflow coefficients of the free water storage to groundwater relationships	-	0-0.4
KSS	Outflow coefficients of the free water storage to interflow relationships	-	0-0.6
C_nh	Scale factor for Manning's roughness coefficient for hillslope routing	-	0-1
C_nr	Scale factor for Manning's roughness coefficient for channel routing	-	0-1
C_twidth	Coefficient to account for the difference between the hypothetical sub-channel network and real tributary network	-	0.1-10.0

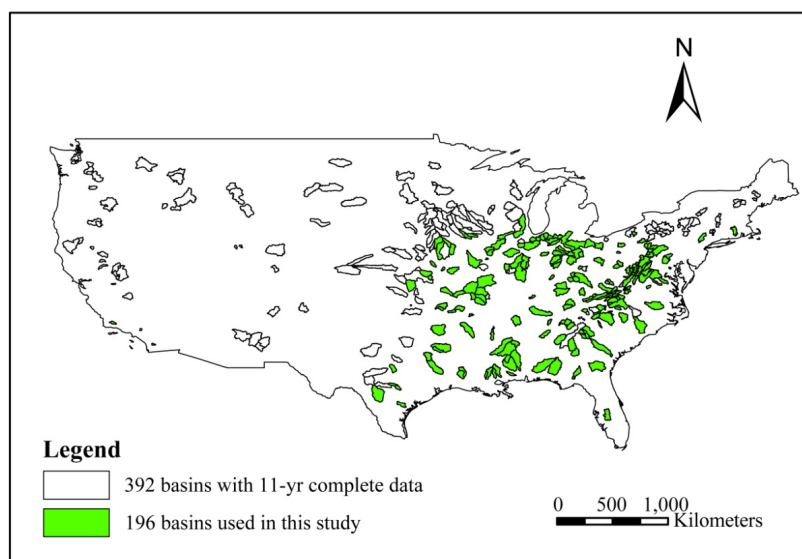
147 3.2 Study area and data

148 The Model Parameter Estimation Experiment (MOPEX) watersheds were chosen as the study
 149 areas. The MOPEX dataset was described by Duan et al. (2006) and can be downloaded from
 150 http://www.nws.noaa.gov/oh/mopex/mo_datasets.htm. Daily mean areal precipitation, potential
 151 evaporation, and streamflow are available for 438 watersheds ranging from 67 to 10329 km²
 152 across the United States. As shown in Kollat et al. (2012), 392 of the MOPEX watersheds have 11
 153 complete years of data from 1 Oct. 1961 to 30 Sep. 1972. Among these watersheds, 196
 154 watersheds across the eastern United States (shown in Figure 1) were selected because of the
 155 applicability of the Xinanjiang hydrological model. Daily precipitation and potential evaporation
 156 were used to drive the hydrological model. Daily streamflow series were used to calibrate the



157 hydrological model. The periods of 1 Oct. 1961 - 30 Sep. 1962, 1 Oct. 1962 - 30 Sep. 1972, and 1
158 Oct. 1972 - 30 Sep. 1982 were selected for warm-up, model calibration, and validation
159 respectively.

160 Faustini et al. (2009) developed the downstream hydraulic geometry relationships for
161 bankfull channel width as a function of drainage area for nine aggregate eco-regions comprising
162 the conterminous United States using 1588 sites from the US Environmental Protection Agency's
163 National Wadeable Streams Assessment. Using these relationships, we calculated the bankfull
164 width for each watershed in this study. The channel slope, sub-channel slope, and drainage density
165 were calculated based on the National Hydrography Plus Dataset (NHDPlus) which is a
166 geo-spatial, hydrologic framework dataset incorporating the National Hydrography Dataset
167 (NDH), the National Elevation Dataset (NED), and the Watershed Boundary Dataset (WBD), and
168 can be downloaded from <http://www.horizon-systems.com/NHDPlus/index.php>. In this study, the
169 minimum slope was set to 0.005%. The main channel was defined as the channel draining out of
170 the watershed outlet and/or into the downstream watershed. Following Eqns. (6) and (8) in Li et al.
171 [2013], the length and width of hypothetical sub-network channel were estimated based on the
172 drainage density value derived from NHDPlus and the aforementioned hydraulic geometry
173 relationships.



174

175 Figure 1. Map of the 196 MOPEX watersheds used in this study. These watersheds were selected from
176 the 392 watersheds with 11 years of data [Kollat et al., 2012].

177 3.3 Optimization algorithm

178 The Epsilon Dominance Nondominated Sorted Genetic Algorithm-II (ϵ -NSGAI) (Kollat and
179 Reed, 2006) was chosen as the optimization algorithm for model calibration in this study. The
180 ϵ -NSGAI integrates epsilon dominance strategy (Laumanns et al., 2002) and automatic
181 parameterization (Reed et al., 2003) with the NSGA-II (Deb et al., 2002). The algorithm has been
182 frequently used in hydrological modeling and has been demonstrated to be consistently better
183 compared to other state-of-the-art evolutionary algorithms (Kollat and Reed, 2006; Sun et al.,
184 2014; Tang et al., 2006).

185 3.4 Evaluation framework

186 According to Kollat et al. (2012), four widely used objective functions focusing on peak flows,



187 low flows, water balance, and flashiness, respectively, were applied in this study. The first one is
 188 Nash-Sutcliffe Efficiency (NSE) (Nash and Sutcliffe, 1970) which emphasizes peak flows, as
 189 shown in Eq. (2),

$$190 \quad NSE = 1 - \frac{\sum_{t=1}^n (Q_{s,t} - Q_{o,t})^2}{\sum_{t=1}^n (Q_{o,t} - \bar{Q}_o)^2} \quad (2)$$

191 where, \bar{Q}_o is the mean observed streamflow over the entire simulation period of length n .

192 The second objective is Transformed Root Mean Square Error (TRMSE) which emphasizes
 193 low flows, as shown in Eq. (3),

$$194 \quad TRMSE = \sqrt{\frac{1}{n} \sum_{t=1}^n (Q'_{s,t} - Q'_{o,t})^2}, \text{ where } Q' = \frac{(1+Q)^\lambda - 1}{\lambda} \quad (3)$$

195 where, $Q'_{s,t}$ is the Box-Cox transformed (Box and Cox, 1964) simulated streamflow at time t ,
 196 $Q'_{o,t}$ is the Box-Cox transformed observed streamflow at time t , Q' is the Box-Cox
 197 transformation of the streamflow Q , λ is a constant ($\lambda = 0.3$).

198 The third objective is Runoff Coefficient Percent Error (ROCE) which emphasizes water
 199 balance, as shown in Eq. (4),

$$200 \quad ROCE = \frac{1}{Y} \sum_{y=1}^Y \left| \frac{\overline{Q_{s,y}}}{\overline{Q_{o,y}}} - 1 \right| \times 100\% \quad (4)$$

201 where, $\overline{Q_{s,y}}$ is the mean annual simulated streamflow, $\overline{Q_{o,y}}$ is the mean annual observed
 202 streamflow, Y is the number of years in the simulation period.

203 The fourth objective is Slope of the Flow Duration Curve (SFDCE) which emphasizes
 204 flashiness of the hydrological response, as shown in Eq. (5),

$$205 \quad SFDCE = \left| \frac{Q_{s,67\%} - Q_{s,33\%}}{Q_{o,67\%} - Q_{o,33\%}} - 1 \right| \times 100\% \quad (5)$$



206 where, $Q_{s,67\%}$ and $Q_{s,33\%}$ are the 67th and 33rd percentile of the simulated streamflow, $Q_{o,67\%}$
207 and $Q_{o,33\%}$ are the 67th and 33rd percentile of the observed streamflow.

208 Price et al. (2012) provided an aggregated multi-objective functions termed the composite
209 likelihood index (CL) compositing three metrics in order to allow trade-offs in fitting high flow,
210 low flow, and flow variability components. In this study, Price et al.'s principle (2012) was applied
211 to aggregate these four selected objective functions described above for evaluating the proposed
212 objective function with different exponent values. Following the process in Price et al. (2012), we
213 first transformed the four objective functions to a similar scale for aggregation, as shown in Eq.
214 (6),

$$\begin{aligned}
 \theta_{NSE} &= \frac{\max(0, NSE_i)}{\sum_{i=1}^L \max(0, NSE_i)} \\
 \theta_{TRMSE} &= \frac{1 - \min(1, |1 - TRMSE_i|)}{\sum_{i=1}^L [1 - \min(1, |1 - TRMSE_i|)]} \\
 \theta_{ROCE} &= \frac{1 - \min(1, |1 - ROCE_i|)}{\sum_{i=1}^L [1 - \min(1, |1 - ROCE_i|)]} \\
 \theta_{SFDCE} &= \frac{1 - \min(1, |1 - SFDCE_i|)}{\sum_{i=1}^L [1 - \min(1, |1 - SFDCE_i|)]}
 \end{aligned} \tag{6}$$

216 where, $\theta_{NSE}, \theta_{TRMSE}, \theta_{ROCE}, \theta_{SFDCE}$ are the scaled $NSE, TRMSE, ROCE, SFDCE$, respectively;
217 the subscript i represents each calibration run with different exponent value of the proposed
218 objective function. L is the total number of calibration runs, which is 9 in this study (see Section
219 3.5). Then CL equally weights these four scaled objective functions, as shown in Eq. (7),

$$CL = \text{mean}(\theta_{NSE}, \theta_{TRMSE}, \theta_{ROCE}, \theta_{SFDCE}) \tag{7}$$

221 3.5 Framework to search for an optimized single-objective function

222 In order to investigate the possibility of using the proposed single-objective function to



223 compromise the multi-response modes of hydrograph, four experiments were designed in this
224 study. The purpose of the first experiment is to identify the OEV for each of 196 MOPEX
225 watersheds, which is the prerequisite for application of the proposed objective function. In this
226 study, we designed nine numbers quasi-uniformly distributed in the range of exponent values
227 [0-2.0] (see Section 2), 0.1, 0.3, 0.5, 0.7, 1.0, 1.3, 1.5, 1.7, and 2.0. For each MOPEX watershed, 9
228 automatic calibrations were conducted with the objective function defined using the 9 exponent
229 values respectively. The OEV was then identified as the exponent value corresponding to the
230 optimal value of CL defined in Section 3.4.

231 According to the identified OEVs, 196 MOPEX watersheds could be grouped into 9
232 categories. We selected one representative watershed from each category for further exploration.
233 In the context of single-objective calibration, the second experiment was implemented to compare
234 the OSOF with the most widely used objective function NSE. Then in the third experiment, we did
235 a comparative study between single-objective calibration with the OSOF and multi-objective
236 calibration with four objective functions described in Section 3.4. Finally, in the fourth experiment,
237 in order to investigate the robustness of calibration with the OSOF, the simulated streamflow was
238 validated in a period of 10 years. We also compared the hydrograph replicating capability of
239 optimized parameters using single-objective calibration and multi-objective calibration in the
240 fourth experiment.

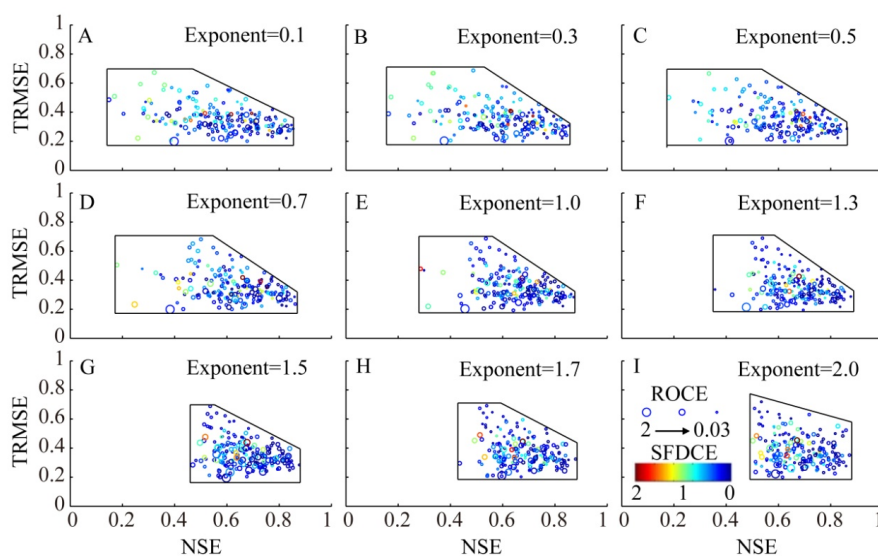
241 **4. Results and discussion**

242 **4.1 Single-objective calibration**

243 Figure 2 shows the results of 196×9 single-objective calibrations in the first experiment. In order



244 to investigate the effect of exponent values on the result of single-objective calibration, four
245 widely used metrics, i.e., NSE, TRMSE, ROCE, and SFDCE, were adopted to evaluate 9
246 optimized simulations for each of 196 MOPEX watersheds.



247
248 Figure 2. The evaluation merits for single-objective calibration. Each sub-figure represents the results
249 calibrated by one exponent value but for all the 196 watersheds. NSE was plotted on the horizontal axis,
250 TRMSE was plotted on the vertical axis, ROCE was plotted as the diameter of circles, SFDCE was
251 plotted as color. A-I represent results with different exponent values. The shapes enclosed by the black
252 envelop lines show the distribution range of the results.

253 From Figure 2(I) to Figure 2(A), as the exponent value decreases from 2.0 to 0.1 the
254 distribution range of NSE increases significantly from 0.5-0.9 to 0.15-0.86. The larger the
255 exponent value is, the better (high score and narrow range) the NSE evaluation merit becomes.
256 This indicates that the objective function with larger exponent value tends to match high flows.
257 For the TRMSE (more related to low flow), its distribution ranges are almost unchanged with
258 different exponent values. The average TRMSEs of 196 watersheds for nine exponent cases were



259 calculated and shown in Figure 2. When the exponent decreases from 2.0 to 0.1, the average
260 TRMSE decreases from 0.386 to 0.351. Also, the proportion of the TRMSE greater than 0.4
261 (worse performance) was calculated for each figure, which also shows a decreasing trend from
262 37.3% to 21.8%. These distribution characteristics of TRMSE show that the simulations of low
263 flows are improved when the exponent value decreases. As the TRMSE tends to concentrate on
264 lower portions, this demonstrates that the objective function with lower exponent value
265 emphasizes low flows. With respect to ROCE and SFDCE, there is no obvious trend detected from
266 the figures. The general performances of ROCE and SFDCE are reasonably well for most
267 calibrations in this study.

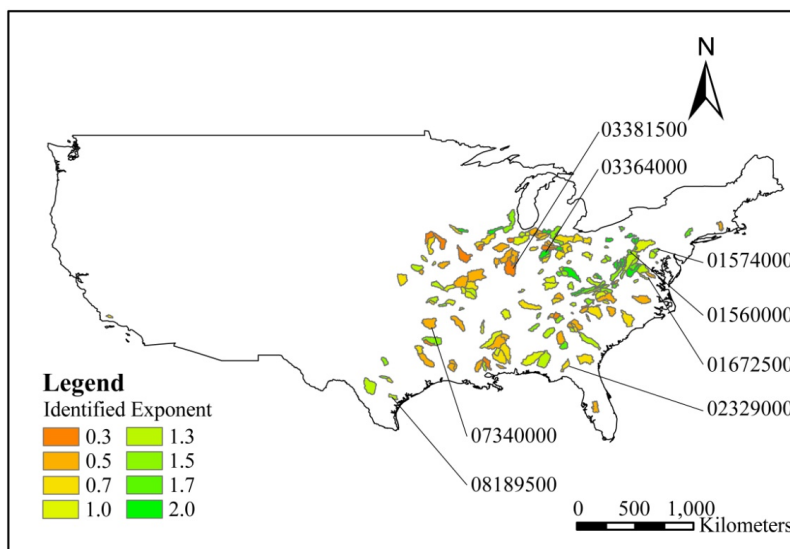
268 In Figure 2(I), many results fall in the bottom right corner, which means that they have a
269 sound simulation for both high flows and low flows. In addition, the other two metrics
270 emphasizing water balance and flashiness of hydrological response are also reasonable. For these
271 watersheds, the objective function with exponent of 2.0 is suitable. However, there are many other
272 watersheds with good simulation of high flows at the expense of poor simulation of low flows,
273 which indicates that NSE is not a reasonable objective function for all kinds of watersheds (also
274 see the discussion in Schaefli and Gupta, 2007).

275 The shapes enclosed by envelop lines of the distribution ranges were also plotted in Figure 2.
276 We found that the right sides of the shapes in Figure 2(A)-(F) are narrower than those in Figure
277 2(G)-(I), which means that some simulations of the watersheds with sound NSE and poor TRMSE
278 are improved when the exponents are moderately adjusted. Especially in Figure 2(C)-(G), many
279 results concentrate in the bottom right corner, indicating that the hypothesis that a proper exponent
280 value can compromise multi-response modes of the hydrograph be reasonable.



281 **4.2 The proposed objective function with the optimal exponent value**

282 The results of single-objective calibration discussed above are evaluated by the composite
283 likelihood index to identify the OEV for each watershed. Figure 3 shows the identified OEVs of
284 the proposed objective function for the 196 MOPEX watersheds. Most of the watersheds with
285 lower OEVs locate in the northwest region, while the watersheds with larger OEVs generally
286 locate in the northeast region. According to the identified OEVs, these watersheds were grouped
287 into eight categories, and then eight representative watersheds were arbitrarily selected from these
288 categories as shown in Figure 3.

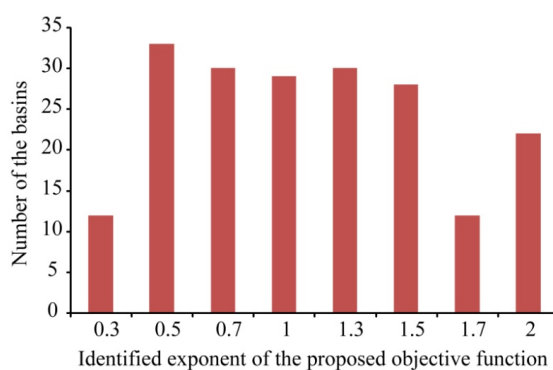


289
290 Figure 3. The optimal exponent values of the proposed objective function for the 196 MOPEX
291 watersheds. Labels are provided for eight watersheds selected as representative watersheds to be
292 explored in detail based on the identified OEVs.

293 Figure 4 shows the histogram of these identified OEVs. Identified OEVs distribute from 0.3
294 to 2.0. For 22 of the 196 MOPEX watersheds, the objective function with exponent of 2.0 is the



295 optimal, which are all located in the bottom right corner of Figure 2(I) with sound simulations of
296 high flows and low flows, as well as water balance and flashiness of hydrological response. Most
297 watersheds tend to prefer the OEV of 0.5, 0.7, 1.0, 1.3, and 1.5. There are also 12 watersheds with
298 OEV of 0.3. The regional distribution of these watersheds concentrate in northwest as shown in
299 Figure 3.



300
301

Figure 4. Histogram of identified OEVs.

302 4.3 Comparison between the proposed objective function and NSE

303 In the context of single-objective calibration, NSE is a traditionally widely used objective function.
304 In order to verify the advantage of the proposed objective function, we compared the OSOF and
305 NSE. Figure 5 shows the results of comparative study at eight representative watersheds. To be
306 noted, the identified OEV is the same as NSE in the watershed 01560000. As shown in Figure
307 5(A1) and 5(A2), we found that the results using the proposed objective function with exponent of
308 2.0 (similar to NSE) are much better in both high flows and low flows when compared to that with
309 exponent of 1.0 which is arbitrarily selected. Other figures on the left side show that the
310 simulations of high flows calibrated by the OSOF have little impact on replicating high flows
311 when compared to NSE. However, focusing on the low flows as shown in the right figures with



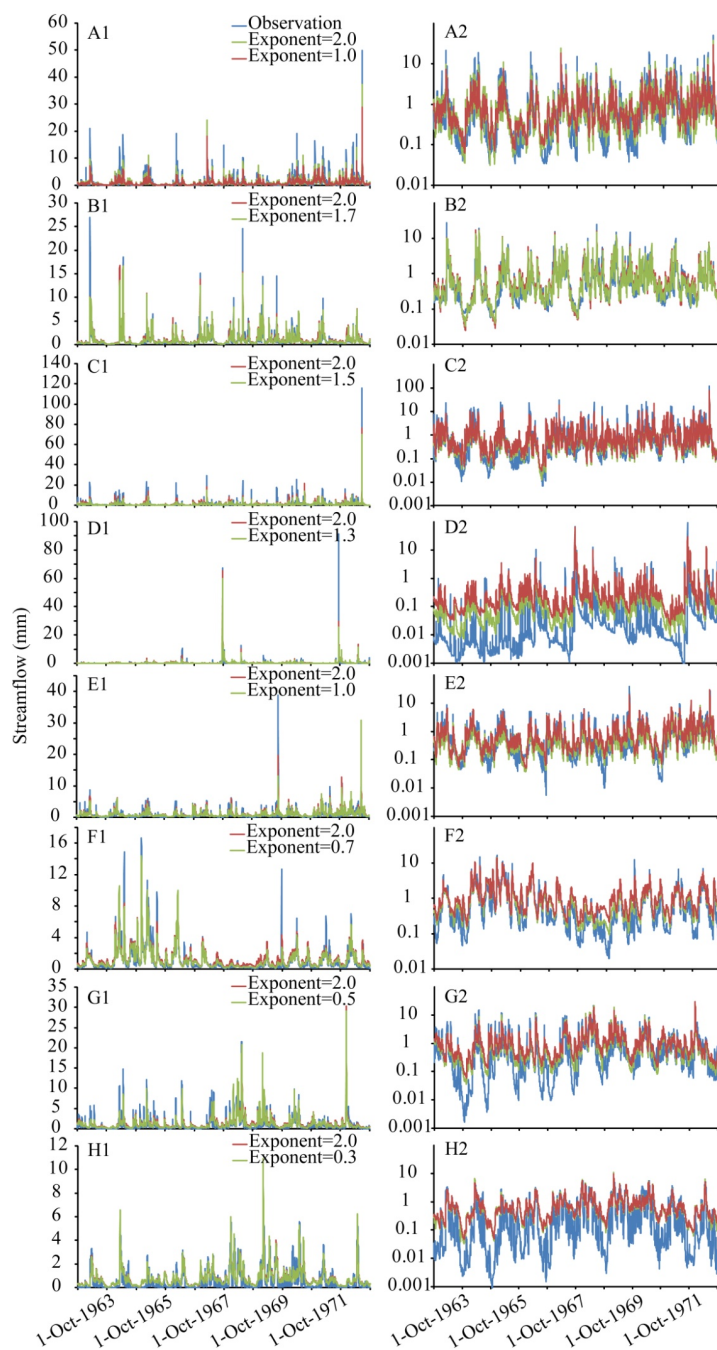
312 logarithmic vertical axis, the calibration with the OSOF significantly improve the simulations
 313 especially in Figure 5(D2) to 5(G2). Four widely used metrics including NSE, TRMSE, ROCE
 314 and SFDCE, were applied to quantitatively analyze the difference between the results using two
 315 objective functions. Table 2 shows that the OSOF simultaneously improves TRMSE, ROCE, and
 316 SFDCE with a slight impairment on NSE at most watersheds, except for watershed 02329000. All
 317 the results indicate that there does exist a single-objective function (OSOF here) that can
 318 compromise multi-response modes of hydrograph, which is usually not the traditionally used
 319 single-objective function NSE.

320 Table 2. Evaluation merits of the simulations calibrated by the optimal single-objective function

321 (OSOF) and NSE

ID of Watersheds	OSOF				NSE			
	NSE	TRMSE	ROCE	SFDCE	NSE	TRMSE	ROCE	SFDCE
01560000	0.640	0.495	0.093	0.093	0.640	0.495	0.093	0.093
03364000	0.787	0.247	0.121	0.039	0.806	0.277	0.255	0.243
01574000	0.679	0.456	0.092	0.021	0.692	0.504	0.174	0.219
08189500	0.652	0.345	1.510	5.897	0.655	0.388	2.997	7.468
01672500	0.615	0.320	0.118	0.096	0.642	0.385	0.356	0.549
02329000	0.848	0.253	0.186	0.155	0.854	0.335	0.548	0.046
07340000	0.726	0.367	0.088	0.141	0.734	0.438	0.256	0.285
03381500	0.714	0.326	0.471	0.017	0.720	0.341	0.503	0.018

322



323
 324 Figure 5. Comparison between the results using proposed objective function and NSE in the calibration
 325 period for 8 representative watersheds. The vertical axis of the four figures in the right column is



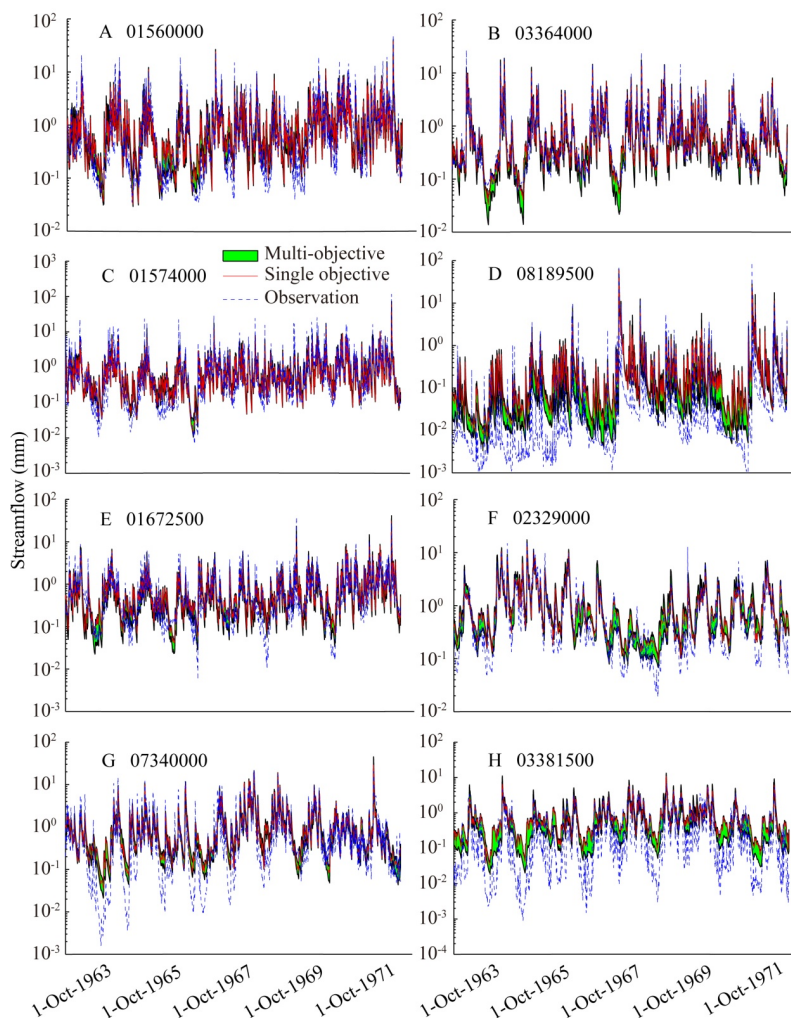
326 logarithmic. From A-H, the identified OEVs decrease from 2.0 to 0.3, the IDs of these watersheds are
327 01560000, 03364000, 01574000, 08189500, 01672500, 02329000, 07340000, and 03381500,
328 respectively. Specifically, for A1 and A2, the proposed objective function is same as NSE, we randomly
329 selected the result with exponent of 1.0 for comparison.

330 **4.4 Comparison between single-objective calibration and multi-objective calibration**

331 Figure 6 compares single-objective calibration with the OSOF and multi-objective calibration with
332 four widely used objective functions in the calibration period at eight representative watersheds.
333 At all these watersheds, the simulation of OSOF calibration locates in the hydrograph ranges
334 enclosed by the envelop lines of Pareto results using multi-objective calibration and can be able to
335 capture the major variability of the hydrograph. In Figure 6(A), 6(C), 6(E) and 6(G), the
336 hydrograph ranges are so narrow that the difference between the results of single-objective
337 function and multi-objective functions can be ignored. It means that at these watersheds
338 multi-objective calibration does not extract more information from historical data. Figure 7(A)
339 shows the flow duration curves (FDCs) at watershed 01574000 (the same as Figure 6(C)). The
340 uncertainty of the streamflow frequency distribution is also obvious smaller than that in the other
341 two watersheds in Figure 7. In Figure 6(B), the simulation using the OSOF calibration is near to
342 the upper bound of uncertainty zone at low flow portions, and the observed hydrograph especially
343 for low flows is generally slightly greater than the simulations. Similarly, in Figure 7(B), the
344 simulated FDC using single-objective calibration almost replicates the observed FDC. It also
345 means that the uncertainty bound using multi-objective calibration does not provide useful
346 information in this case. On the contrary, in Figure 6(D), 6(F), and 6(H), results of multi-objective



347 calibration contain some simulations which can better capture the variability of the streamflow,
348 but the best simulations in the hydrograph ranges are also far away from the observation
349 especially for low flows. Corresponding to Figure 6(H), Figure 7(C) shows the similar results
350 from the perspective of frequency distribution. For example, the 80th percentile of the lower bound
351 of Pareto results is 0.09 mm, while that of the observed streamflow is 0.02 mm. Overall,
352 single-objective calibration with the OSOF can compromise multi-response modes of the
353 hydrograph to obtain a relatively sound simulation, which is comparable to the result of
354 multi-objective calibration.



355

356

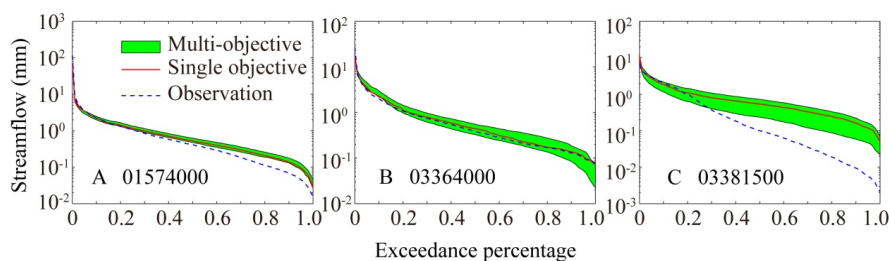
357

358

359

Figure 6. Comparison between the results using single objective calibration with the optimal single-objective function and multi-objective calibration with four widely used objective functions in the calibration period for 8 representative watersheds. The vertical axis of the figure is logarithmic.

From A-H, the identified optimal exponent value decreases from 2.0 to 0.3.



360

361 Figure 7. Observed and simulated flow duration curves (FDCs) for 3 representative watersheds. The

362

vertical axis of the figure is logarithmic.

363 4.5 Model validation

364 The above analyses demonstrate that the proposed OSOF is effective during the calibration period.

365 In this section, we aimed to test its robustness by comparing the performance of single-objective

366 calibration with OSOF to that of multi-objective calibration during the validation period. The

367 simulations using OSOF calibration can also capture the major patterns of the hydrograph during

368 the validation period as shown in Figure 8. Similar to the results during the calibration period

369 (Figure 6), in Figure 8(A), 8(B), 8(C), 8(E), and 8(G), the hydrograph ranges in the validation

370 period are also narrow, which means that not only in the calibration period can the results of

371 OSOF calibration be comparable to that of multi-objective calibration, but also in the validation

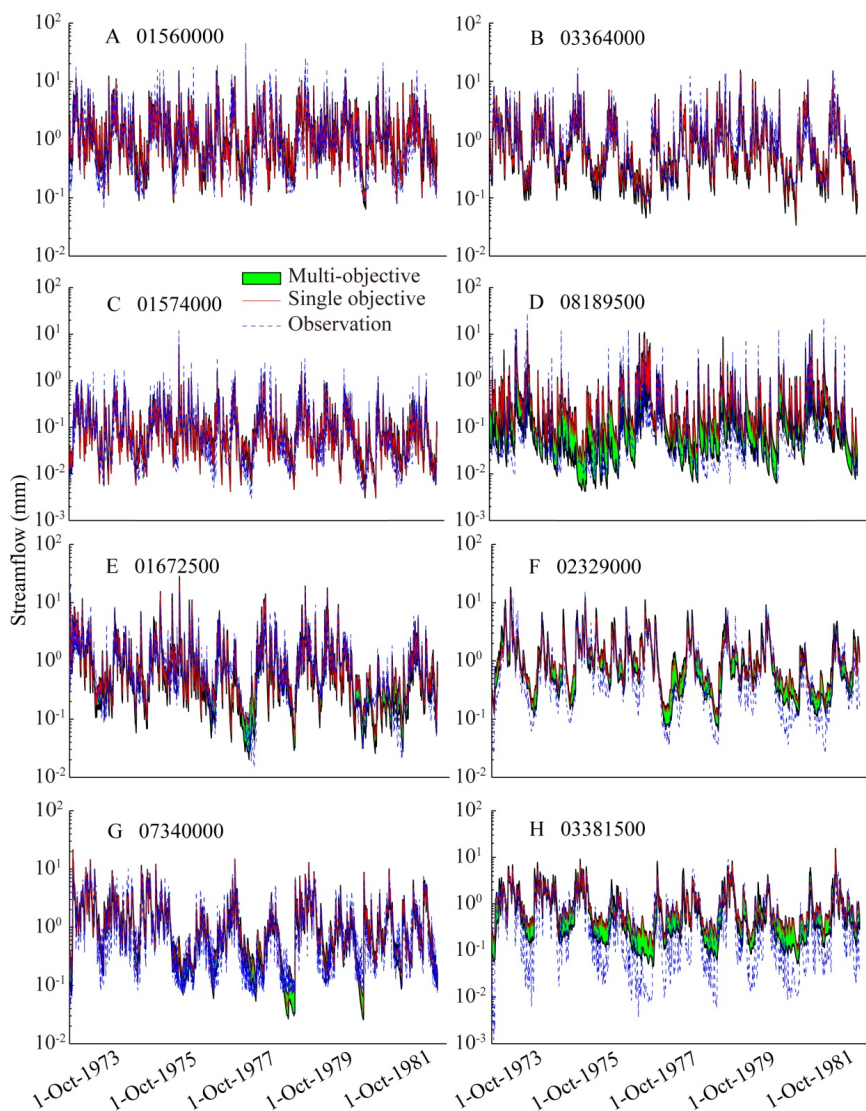
372 period at these watersheds. At the other three watersheds, multi-objective calibration provides

373 more useful information about the hydrograph, but there is also a wide gap between the best

374 simulations in the hydrograph ranges and the observations. In general, parameter set identified by

375 the proposed optimal single-objective function has a robust performance in hydrological

376 modeling.



377

378 Figure 8. Comparison between the results using single objective calibration with the proposed objective

379 function and multi-objective calibration with four widely used objective functions in the validation

380 period for 8 representative watersheds. The vertical axis of the figure is logarithmic. From A-H, the

381

identified optimal exponent values decrease from 2.0 to 0.3.



382 **5. Discussion and Conclusions**

383 In this study, we proposed a new methodology that can compromise multi-response modes (i.e.,
384 multi-objective functions) of the hydrograph by using an optimized single-objective function. The
385 single-objective function is generally defined as a power function of the absolute error between
386 observed and simulated streamflow, and the exponent of power function is then optimized when
387 applying to a specific watershed. The methodology was applied to 196 model parameter
388 estimation experiment (MOPEX) watersheds across the eastern United States using Xinanjiang
389 model. The optimal exponent value for each watershed was obtained by targeting four popular
390 objective functions focusing on peak flows, low flows, water balance, and flashiness, respectively.
391 The results show that the optimal single-objective function can achieve a better hydrograph
392 simulation compared to traditional Nash-Sutcliffe efficiency for most watersheds, as well as can
393 balance high flow part and low flow part of the hydrograph to be comparable to multi-objective
394 calibration. Our work demonstrates the potential of single-objective function to simultaneously
395 address multi-response modes of the hydrograph.

396 Multi-objective calibration is based on the concept of Pareto optimal, which defines the
397 improvement strictly as that given an initial solution, a change to a better solution results in
398 making at least one objective function better without making any other objective function worse.
399 Actually, as discussed in Tekleab et al. (2011), modelers may be willing to accept suboptimal
400 performance of one aspect of the streamflow series in order to improve accuracy in one or more
401 other aspects. The proposed optimal single-objective function in this study essentially relaxes the
402 strict definition of Pareto optimal. For example, when compared to NSE, the proposed OSOF
403 improves two or three objective functions which represent corresponding modes of hydrological



404 responses at a slight expense of the simulation of high flows, which is not Pareto improvement.
405 Kollat et al. (2012) found that the meaningful multi-objective trade-offs are far less frequent than
406 prior literature has suggested. They introduced the concept of epsilon-dominance, a way to relax
407 the Pareto optimal, to obtain meaningful results, and identified only one solution at many MOPEX
408 watersheds. While multi-objective calibration is helpful to address multi-modes, single-objective
409 calibration with a proper objective function can also identify a good compromise solution against
410 multiple criteria which would be applicable for hydrological planning and management.

411 In addition, automatic calibration (whether single-objective or multi-objective) of
412 hydrological models is usually implemented with the same objective function or combination of
413 objective functions for different watersheds. However, we may expect different objective
414 functions for watersheds with significant differences in terms of climatic condition, vegetation
415 cover, land use/cover, soil texture, etc. This study demonstrates this idea by identifying a specific
416 objective function for a specific watershed.

417 Theoretically, the proposed methodology utilizes the trade-off on the exponent value of
418 power function to substitute for the trade-offs on multiple objectives. It could be practically
419 adopted in the hydrological modeling if the optimized exponent could be determined *a priori*
420 according to hydrological/climatic/landscape characteristics in a specific watershed. In the
421 following study, an empirical equation is expected to be established to relate the optimal exponent
422 value of the proposed objective function with some watershed and hydrograph indices or a
423 combination of these indices.



424 **Acknowledgements**

425 This work has been funded by the National Science Foundation of China (NSFC 51190092,
426 U1202232), the foundation of State Key Laboratory of Hydrosience and Engineering of Tsinghua
427 University (2016-KY-03). H. Li was supported by the Office of Science of the U.S. Department of
428 Energy as part of the Earth System Modeling Program. Their supports are greatly appreciated. The
429 Pacific Northwest National Laboratory is operated by Battelle for the U.S. Department of Energy
430 under Contract DE-AC05-76RLO1830.
431



432 **References**

- 433 Bao, H.J. et al., 2011. Coupling ensemble weather predictions based on TIGGE database with
434 Grid-Xinjiang model for flood forecast. *Advances in Geosciences*, 29: 61-67.
- 435 Bekele, E.G., Nicklow, J.W., 2007. Multi-objective automatic calibration of SWAT using NSGA-II.
436 *Journal of Hydrology*, 341(3-4): 165-176.
- 437 Booij, M.J., Krol, M.S., 2010. Balance between calibration objectives in a conceptual hydrological
438 model. *Hydrological Sciences Journal*, 55(6): 1017-1032.
- 439 Box, G.E.P., Cox, D.R., 1964. An analysis of transformations. *Journal of the Royal Statistical*
440 *Society. Series B*, 26(2): 211-252.
- 441 Boyle, D.P., Gupta, H.V., Sorooshian, S., 2000. Toward improved calibration of hydrologic
442 models: Combining the strengths of manual and automatic methods. *Water Resources Research*,
443 36(12): 3663-3674.
- 444 Cheng, C.-T., Zhao, M.-Y., Chau, K.W., Wu, X.-Y., 2006. Using genetic algorithm and TOPSIS
445 for Xinjiang model calibration with a single procedure. *Journal of Hydrology*, 316(1-4):
446 129-140.
- 447 Deb, K., Pratap, A., Agarwal, S., Meyarivan, T., 2002. A fast and elitist multiobjective genetic
448 algorithm: NSGA-II. *IEEE Transactions on Evolutionary Computation*, 6(2): 182-197.
- 449 Duan, Q. et al., 2006. Model Parameter Estimation Experiment (MOPEX): An overview of
450 science strategy and major results from the second and third workshops. *Journal of Hydrology*,
451 320(1-2): 3-17.
- 452 Efstratiadis, A., Koutsoyiannis, D., 2010. One decade of multi-objective calibration approaches in
453 hydrological modelling: a review. *Hydrological Sciences Journal*, 55(1): 58-78.



- 454 Faustini, J.M., Kaufmann, P.R., Herlihy, A.T., 2009. Downstream variation in bankfull width of
455 wadeable streams across the conterminous United States. *Geomorphology*, 108(3-4): 292-311.
- 456 Fenicia, F., Savenije, H.H.G., Matgen, P., Pfister, L., 2007. A comparison of alternative
457 multiobjective calibration strategies for hydrological modeling. *Water Resources Research*,
458 43(3): 93-108.
- 459 Gan, T.Y., Dlamini, E.M., Biftu, G.F., 1997. Effects of model complexity and structure, data
460 quality, and objective functions on hydrologic modeling. *Journal of Hydrology*, 192(1-4):
461 81-103.
- 462 Gill, M.K., Kaheil, Y.H., Khalil, A., McKee, M., Bastidas, L., 2006. Multiobjective particle swarm
463 optimization for parameter estimation in hydrology. *Water Resources Research*, 42(7):
464 257-271.
- 465 Guinot, V., Cappelaere, B., Delenne, C., Ruelland, D., 2011. Towards improved criteria for
466 hydrological model calibration: theoretical analysis of distance- and weak form-based
467 functions. *Journal of Hydrology*, 401(1-2): 1-13.
- 468 Gupta, H.V., Kling, H., Yilmaz, K.K., Martinez, G.F., 2009. Decomposition of the mean squared
469 error and NSE performance criteria: Implications for improving hydrological modelling.
470 *Journal of Hydrology*, 377(1-2): 80-91.
- 471 Gupta, H.V., Sorooshian, S., Yapo, P.O., 1998. Toward improved calibration of hydrologic models:
472 Multiple and noncommensurable measures of information. *Water Resources Research*, 34(4):
473 751-763.
- 474 Hall, J., W., Tarantola, S., Bates, P., D., Horritt, M., S., 2005. Distributed sensitivity analysis of
475 flood inundation model calibration. *Journal of Hydrologic Engineering*, 131(2): 117-126.



- 476 Jain, S.K., Sudheer, K.P., 2008. Fitting of hydrologic models: a close look at the Nash-Sutcliffe
477 index. *Journal of Hydrologic Engineering*, 13: 981-986.
- 478 Ju, Q. et al., 2009. Division-based rainfall-runoff simulations with BP neural networks and
479 Xinanjiang model. *Neurocomputing*, 72(13-15): 2873-2883.
- 480 Khu, S.-T., Madsen, H., di Pierro, F., 2008. Incorporating multiple observations for distributed
481 hydrologic model calibration: An approach using a multi-objective evolutionary algorithm and
482 clustering. *Advances in Water Resources*, 31(10): 1387-1398.
- 483 Kollat, J.B., Reed, P.M., 2006. Comparing state-of-the-art evolutionary multi-objective algorithms
484 for long-term groundwater monitoring design. *Advances in Water Resources*, 29(6): 792-807.
- 485 Kollat, J.B., Reed, P.M., Wagener, T., 2012. When are multiobjective calibration trade-offs in
486 hydrologic models meaningful? *Water Resources Research*, 48(3): 221-239.
- 487 Krause, P., Boyle, D.P., Bäse, F., 2005. Comparison of different efficiency criteria for hydrological
488 model assessment. *Advances in Geosciences*, 5: 89-97.
- 489 Laumanns, M., Thiele, L., Deb, K., Zitzler, E., 2002. Combining convergence and diversity in
490 evolutionary multiobjective optimization. *Evolutionary Computation*, 10(3): 263-282.
- 491 Li, H. et al., 2013. A Physically Based Runoff Routing Model for Land Surface and Earth System
492 Models. *Journal of Hydrometeorology*, 14(3): 808-828.
- 493 Li, H., Zhang, Y., Chiew, F.H.S., Xu, S., 2009. Predicting runoff in ungauged catchments by using
494 Xinanjiang model with MODIS leaf area index. *Journal of Hydrology*, 370(1-4): 155-162.
- 495 Madsen, H., 2000. automatic calibration of a conceptual rainfall-runoff model. *Journal of*
496 *Hydrology*, 235: 276-288.
- 497 Madsen, H., 2003. Parameter estimation in distributed hydrological catchment modelling using



- 498 automatic calibration with multiple objectives. *Advances in Water Resources*, 26: 205-216.
- 499 Madsen, H., Wilson, G., Ammentorp, H., Christian, 2002. Comparison of different automated
- 500 strategies for calibration of rainfall-runoff models. *Journal of Hydrology*, 261: 48-59.
- 501 Matott, L.S., Babendreier, J.E., Purucker, S.T., 2009. Evaluating uncertainty in integrated
- 502 environmental models: A review of concepts and tools. *Water Resources Research*, 45(6):
- 503 735-748.
- 504 McCuen, R.H., Snyder, W.M., Cutter, A.G., 2006. Evaluation of the Nash-Sutcliffe efficiency
- 505 index. *Journal of Hydrologic Engineering*, 11(6): 597-602.
- 506 Muleta, M.K., 2012. Model Performance Sensitivity to Objective Function during Automated
- 507 Calibrations. *Journal of Hydrologic Engineering*, 17(6): 756-767.
- 508 Nash, J.E., Sutcliffe, J.V., 1970. River flow forecasting through conceptual models part I. A
- 509 discussion of principles. *Journal of Hydrology*, 10(3): 282-290.
- 510 Pokhrel, P., Gupta, H.V., 2010. On the use of spatial regularization strategies to improve
- 511 calibration of distributed watershed models. *Water Resources Research*, 46(1): 1-17.
- 512 Price, K., Purucker, S.T., Kraemer, S.R., Babendreier, J.E., 2012. Tradeoffs among watershed
- 513 model calibration targets for parameter estimation. *Water Resources Research*, 48(10):
- 514 136-151.
- 515 Reed, P., Minsker, B.S., Goldberg, D.E., 2003. Simplifying multiobjective optimization: An
- 516 automated design methodology for the nondominated sorted genetic algorithm-II. *Water*
- 517 *Resources Research*, 39(7): 257-271.
- 518 Schaeffli, B., Gupta, H.V., 2007. Do Nash values have value? *Hydrological Processes*, 21:
- 519 2075-2080.



- 520 Sun, Y., Tian, F., Yang, L., Hu, H., 2014. Exploring the spatial variability of contributions from
521 climate variation and change in catchment properties to streamflow decrease in a mesoscale
522 basin by three different methods. *Journal of Hydrology*, 508: 170-180.
- 523 Tang, Y., Reed, P., Wagener, T., 2006. How effective and efficient are multiobjective evolutionary
524 algorithms at hydrologic model calibration? *Hydrology and Earth System Sciences*, 10:
525 289-307.
- 526 Tang, Y., Reed, P.M., Kollat, J.B., 2007. Parallelization strategies for rapid and robust evolutionary
527 multiobjective optimization in water resources applications. *Advances in Water Resources*,
528 30(3): 335-353.
- 529 Tekleab, S. et al., 2011. Water balance modeling of Upper Blue Nile catchments using a top-down
530 approach. *Hydrology and Earth System Sciences*, 15(7): 2179-2193.
- 531 van Griensven, A., Bauwens, W., 2003. Multiobjective autocalibration for semidistributed water
532 quality models. *Water Resources Research*, 39(12): 1348-1357.
- 533 van Werkhoven, K., Wagener, T., Reed, P., Tang, Y., 2009. Sensitivity-guided reduction of
534 parametric dimensionality for multi-objective calibration of watershed models. *Advances in*
535 *Water Resources*, 32(8): 1154-1169.
- 536 Vrugt, J.A., Bouten, W., Gupta, H.V., Sorooshian, S., 2002. Toward improved identifiability of
537 hydrologic model parameters: The information content of experimental data. *Water Resources*
538 *Research*, 38(12): 1312-1324.
- 539 Vrugt, J.A., Gupta, H.V., Bastidas, L.A., Bouten, W., Sorooshian, S., 2003. Effective and efficient
540 algorithm for multiobjective optimization of hydrologic models. *Water Resources Research*,
541 39(8): 1214-1232.



- 542 Wagener, T., 2003. Evaluation of catchment models. *Hydrological Processes*, 17(16): 3375-3378.
- 543 Yapo, P.O., Gupta, H.V., Sorooshian, S., 1998. Multi-objective global optimization for hydrologic
544 models. *Journal of Hydrology*, 204: 83-97.
- 545 Zhao, R.-J., 1992. The Xinanjiang model applied in China. *Journal of Hydrology*, 135: 371-381.
- 546